



**Grainger College  
of Engineering**

UNIVERSITY OF ILLINOIS URBANA-CHAMPAIGN

An Internship Report on  
**Design Validation and Balancing of 4 cylinder,  
Individually Balanced Crankshaft**

AT



Date: 02/06/2025 - 28/07/2025

**Project Guide: Mr. Sajan Abraham**  
(R&D Engine)

Submitted by:  
**Advait Chordia**  
B.S Engineering Mechanics  
& Minor in Materials Science



## **CERTIFICATE**

This is to certify that the Industry Internship Project Report titled “**Design Validation and Balancing of 4 cylinder, Individually Balanced Crankshaft**” is a Bonafide work carried out by Mr. Advait Chordia, a student at the University of Illinois Urbana-Champaign, as a summer internship project in the academic year 2025.

**Mr. Sajan Abraham**  
**Dy. General Manager**  
**R&D Engine Design**  
**Force Motors Limited**

**Mr. Nitin Sheth**  
**Associate Vice President**  
**R&D Powertrain**  
**Force Motors Limited**

## **Table of Contents**

Acknowledgements.....	4
Abstract.....	5
Company Profile .....	6
About the Company .....	6
History of the Company.....	6
Product Range.....	7
Introduction to Crankshaft .....	10
Crankshaft Dynamics in an IC Engine.....	10
Types of Crankshafts.....	11
Fabrication: Forging, Machining & Finishing .....	13
Importance of precision in high-speed operation.....	14
Working Principle .....	15
Crankshaft Design Guideline.....	17
Loading Scenarios During Combustion.....	17
Crankshaft Dimensional Constraints Based on Mechanical Limits .....	18
Crankshaft Balancing.....	28
Principles of Unbalance: Static and Dynamic Balancing .....	28
Assumptions & Notes .....	29
Analytical Model for the balancing of Individually Balanced Crankshaft.....	29
Crankshaft Fatigue Testing for Validation .....	34
Conclusion .....	42

## **Acknowledgements**

I would like to express my sincere appreciation to Force Motors Ltd. for providing me with the opportunity to intern with the Research and Development Department. This internship was an enriching experience, significantly deepening my understanding of practical engineering concepts and directly enhancing my academic and professional growth.

I am particularly grateful to Mr. Sajan Abraham (Deputy General Manager – R&D Engine Design), my project mentor, for his insightful guidance and unwavering support. His practical approach and willingness to share detailed knowledge during my project, "Design and Testing of Individually Balanced Crankshafts," greatly enhanced my understanding of analytical methods and engineering calculations fundamental to dynamic crankshaft balancing and critical design considerations tailored to specific engine performance needs.

I extend my gratitude to Mr. Atish Ovhal (Senior Manager) for generously sharing his expertise and continuously supporting my learning process. His patient explanations about engine components, their functions, and the intricate constraints involved in crankshaft design proved invaluable. His mentorship was instrumental in helping me effectively fulfil my responsibilities and remain focused on my technical objectives.

I also genuinely appreciate the welcoming and supportive atmosphere created by the Management and the entire team at Force Motors Ltd. Experiencing real-world engineering challenges alongside professionals passionate about their work was truly motivating and impactful.

This internship has been an important milestone in my academic and professional journey, and I sincerely thank everyone at Force Motors for their guidance, encouragement, and generosity in sharing their extensive knowledge.

## **Abstract**

The balancing method used for crankshafts significantly impacts engine performance, durability, and assembly flexibility. This project, conducted at Force Motors Ltd., Akurdi Plant, focused on evaluating and demonstrating the advantages of individually (internally) balanced crankshafts compared to traditionally used assembly-balanced crankshafts.

Individually balanced crankshafts utilize counterweights alone, eliminating the dependence on external components like harmonic dampers and flywheels during the balancing process. This method significantly simplifies engine assembly, reduces production time, and facilitates interchangeability of flywheels, providing greater flexibility for future engine modifications.

In contrast, assembly-balanced crankshafts rely on external balancing components at either end, leading to inherent drawbacks such as increased torsional flex at high RPMs due to uneven mass distribution and potential mismatches in stacked parts post-manufacturing. These disadvantages can lead to diminished durability and suboptimal engine performance under demanding operating conditions.

Through theoretical analysis, computational simulations, and empirical testing on prototype engines, this project validated that individually balanced crankshafts effectively mitigate these issues, exhibiting reduced torsional stress, improved dynamic stability, and better adaptability to engine modifications.

The outcomes confirm the feasibility of the individually balanced crankshafts underscore the long-term benefits and feasibility of transitioning toward internally balanced crankshaft designs, highlighting improved engine reliability, performance consistency, and simplified maintenance processes.

# **Company Profile**

## **About the Company**

Force Motors Limited is an Indian multinational, vertically integrated automotive company headquartered in Pune, Maharashtra. The company is a flagship of the Dr. Abhay Firodia Group and is known for its deep expertise in the design, development, and manufacturing of a full spectrum of automotive components, aggregates, and vehicles. A key pillar of its operations is the state-of-the-art research and development in powertrain technology, which has positioned Force Motors as a critical supplier of high-precision engines and axles to several global manufacturers. The company's well-known product brands include the Traveller, Trax, and the Gurkha off-road vehicle. Force Motors maintains a strong domestic presence and exports to various countries in Africa, Latin America, SAARC, and the Gulf.

## **History of the Company**

Force Motors was established in 1958 by Shri. N.K. Firodia with the vision to provide affordable commercial transport for the masses. From its inception until 2005, the company was known as Bajaj Tempo Motors, originating from a joint venture between Bajaj Trading Ltd. and Germany's Tempo. The company was a pioneer in the Indian light commercial vehicle space, introducing the iconic three-wheeled Tempo Hanseat and the Matador, India's first diesel LCV.

Over the decades, Force Motors has built its capabilities through strategic partnerships with global leaders. A long-standing association with Daimler has been a cornerstone of the company's growth, which has included producing engines for Mercedes-Benz cars in India. The company also formed a joint venture with MAN for heavy commercial vehicles, which was later established as a separate concern in 2012. These collaborations have enabled the company to develop in-house expertise and harness advanced technology, cementing its legacy as a key contributor to the Indian automotive industry.

## Product Range

Force Motors offers a diverse portfolio of vehicles designed to meet the needs of passenger transport, commercial logistics, and specialized utility applications. The product range is a testament to the company's vertically integrated manufacturing capabilities.

### Passenger & Commercial Vehicles:



(a)

(b)



(c)

*Figure 1: Images of Passenger & Commercial Vehicle Range (a) Traveller, (b) Monobus, & (c) Urbania*

- a) **Traveller:** The Force Traveller is a fully built minibus with a seating capacity of 25+driver. It is powered by a 2596 cc, 4-cylinder diesel engine that produces 115 hp and 350 Nm of torque. The Traveller features disc brakes on all wheels, ABS, and EBD, making it a popular choice for comfortable and safe group transport.
  
- b) **Monobus:** The Monobus features a lightweight monocoque body for high fuel efficiency and best-in-class safety. It offers seating for 33+driver and is powered by a 2596 cc, 4-cylinder diesel engine with 114 hp and 350 Nm of torque. For passenger comfort and safety, it includes wide seats, hydraulic suspension, and all-wheel hydraulic disc brakes with ABS and EBD.

- c) **Urbania:** The Force Urbania is a next-generation modular monocoque van powered by a 115 hp, 350 Nm Mercedes-derived diesel engines. It sets a new benchmark in its segment with first-in-class crash compliance, dual airbags, and all-wheel disc brakes with ABS and EBD for superior safety and ride comfort.

Special Application & Quick Response Vehicles:



(a)

(b)



(c)

*Figure 2: Images of Special Purpose Range Vehicles (a) Traveller School Bus, (b) Traveller Ambulance, & (c) Trax Police Van*

- **Traveller Range:** The Force Traveller Delivery Van, School Bus and Ambulance Van are a range of vans designed for urban and intercity goods transport. They have a payload capacity of 1464 kg and is powered by a 2596 cc, 4-cylinder diesel engine delivering 114 hp and 350 Nm of torque. The vans are equipped with a 70-litre fuel tank and manual transmission. Above are photos of a few of the mentioned vans.
- **Trax range:** The Trax platform is adapted for emergency services such as fire and rescue, delivery van, school van and Ambulance to name a few. These Quick Response Vehicles feature specialized firefighting and rescue equipment, including storage for extinguishers, ventilators, and other essential tools. Pictured variations include the

Ambulance, Fire brigade, and Police bus. Above are photos of a few of the mentioned vans.

Multiutility Vehicles:



(a)

(b)

*Figure 3: Images of Multiutility Vehicle Range (a) Trax & (b) Gurkha*

- **Trax:** The Force Trax Cruiser is a robust Multiutility Vehicle (MUV) known for its durability and versatility in challenging terrains. With a seating capacity of up to 13, it is powered by a 2569 cc, 4-cylinder diesel engine. It is widely used for both passenger and utility applications, including as a school van, police van, and ambulance.
- **Gurkha:** The Force Gurkha is a 4-seater SUV designed for rugged use and off-road adventures. It is equipped with a 2596 cc, 4-cylinder diesel engine delivering 138 bhp and 320 Nm of torque. Key off-road features include manual locking differentials, a stock snorkel, and a ground clearance of 233 mm.

# Introduction to Crankshaft

## Crankshaft Dynamics in an IC Engine

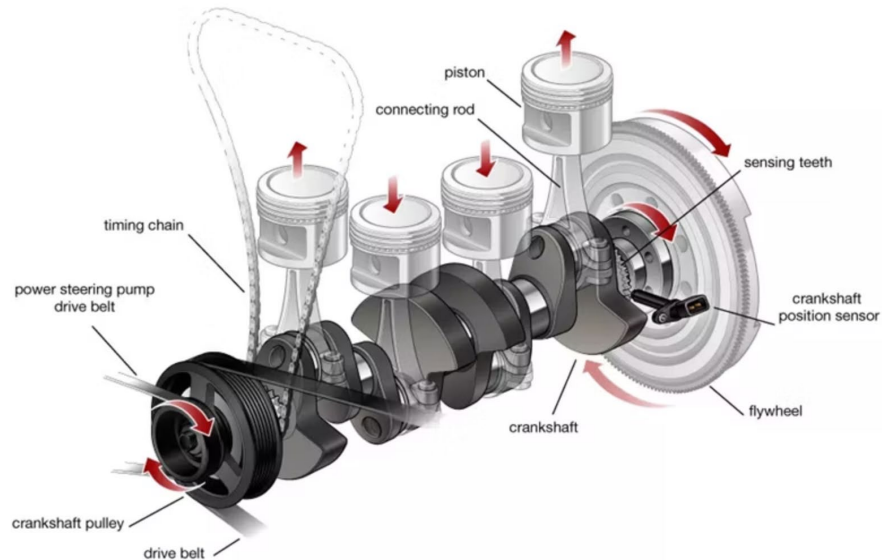


*Figure 4: Image of a Crankshaft*

An internal combustion (IC) diesel engine essentially converts the chemical energy stored in a fuel, diesel in this case, into useful mechanical work. This process begins with the combustion of an air-fuel mixture within the combustion chamber, a precisely machined volume within the engine block, sealed by the cylinder head. The rapid expansion of hot gases from this combustion event exerts immense pressure on the head of the pistons pushing it linearly downwards. This up-and-down motion continues within each piston's respective cylinder. This first step transforms the chemical energy of the fuel into kinetic energy.

To continue the energy transformation, the piston is linked to the crankshaft via a connecting rod (conrod). The crankshaft itself is a complex shaft situated in the lower section of the engine block, supported by main bearings that allow it to rotate freely about its length.

Now closing in on the crankshaft's role, it converts the reciprocating motion of the pistons into the continuous rotary motion that serves as the engine's main mechanical output. Its unique geometry, featuring offset journals known as crankpins where the connecting rods attach, masterfully translates the linear force from the pistons into torque. This rotation is then transferred from the crankshaft, through the flywheel and clutch, to the vehicle's transmission system. The transmission subsequently gears this power up or down to provide the required torque and rotational speed to the wheels.

Beyond this primary function, the crankshaft also is responsible for the engine's overall stability and timing. It also features counterweights to offset the immense rotational and reciprocating forces generated by the crank assembly and pistons, which is critical for smooth operation and minimizing vibration. Additionally, the crankshaft provides the rotational drive for other essential engine systems, most notably the camshaft, ensuring valve timing remains perfectly synchronized with piston movement.

### Types of Crankshafts

#### 1. By Method of Balancing

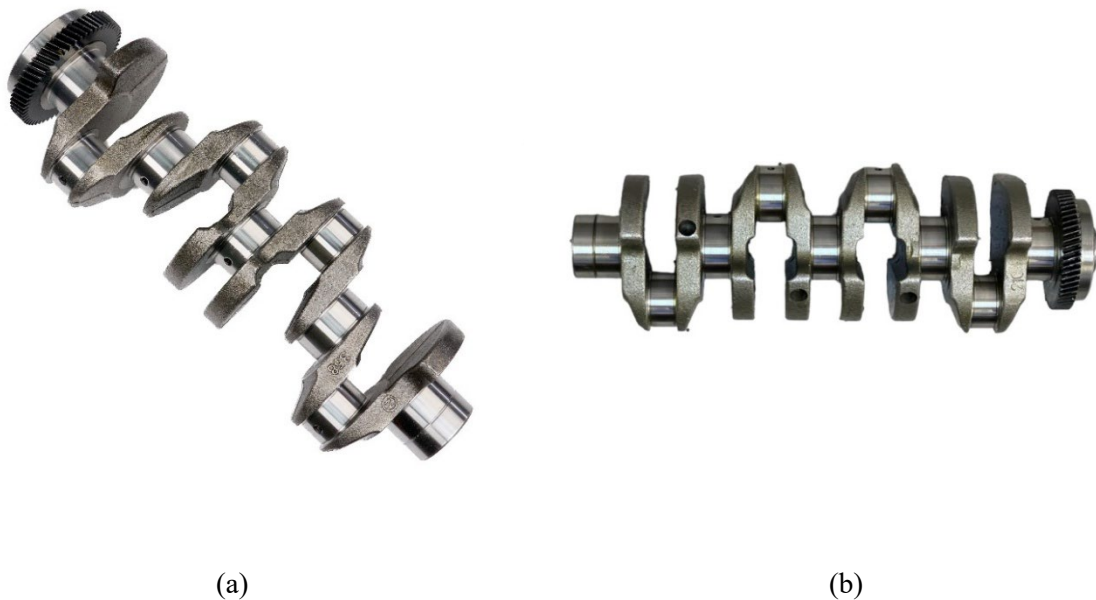


*Figure 5: A pictorial representation of the difference between (a) an assembly balanced and (b) an individually balanced crankshaft*

The strategy for mitigating engine vibration and power loss is critically dependent on how well the crankshaft is balanced. There are primarily two different balancing methods, assembly (externally) balanced or individual (internally) balanced.

**Assembly balancing** treats the entire rotating system—including the crankshaft, harmonic balancer, and flywheel—as a single unit. This method achieves overall equilibrium by spinning the complete assembly and making corrective adjustments, by drilling material from the external components, and is a common approach in many mass-production engines. It possesses an inherent drawback; the primary balancing masses are located at the ends of the shaft, any internal unbalance can cause the crankshaft to experience significant torsional flex, especially at higher RPMs. This internal stress can lead to diminished durability and suboptimal

engine performance. Historically, Force Motors has used this method of manufacturing to produce its crankshafts.

However, for better performance, **Individual (or internal) balancing** is the preferred standard. This meticulous method focuses on perfecting the crankshaft as a standalone, neutrally balanced component, where all the balancing of the forces from the piston and connecting rod is done with precisely engineered counterweights integrated into the crankshaft itself. This approach addresses harmonic vibrations directly at their source and ensures that all the external components, like the flywheel and damper, are also neutrally balanced and thus fully interchangeable. This interchangeability provides greater flexibility for future engine modifications and simplifies the production process, as components do not require balancing after being assembled. This report is concerned exclusively with the design and analysis of these Individually Balanced Crankshafts.

## 2. By Method of Manufacturing



*Figure 6: Crankshaft made via casting (upper) and forging (lower)*

The manufacturing method of a crankshaft is a primary determinant of its performance, durability, and cost, with the three principal methods being casting, forging, and machining from billet.

**Cast crankshafts**, created by pouring molten ductile iron into a die cast, represent the most cost-effective solution and are well-suited for the moderate stress levels found in many mass-produced passenger vehicle engines.

For applications demanding higher strength and fatigue resistance, such as in diesel and high-performance engines, **forged crankshafts** are the standard; this process involves pressing a heated steel billet into a die, which aligns the material's grain structure with the component's

geometry for superior strength. As they provide a good balance between feasibility and performance, this is the method of manufacturing used by FML.

At the highest end of the performance spectrum are **billet crankshafts**, which are CNC machined from a solid block of high-grade steel. While this method offers the ultimate in design precision and material quality, its significant cost in both material waste and machine time reserves it for top-tier motorsports and bespoke engine builds.

### **Fabrication: Forging, Machining & Finishing**

At Force Motors Ltd., crankshafts are forged from high-strength **38MnVs6** alloy steel using closed-die hydraulic presses. Unlike billet crankshafts, which are machined from a solid block of steel, forging compresses heated steel into dies, aligning the internal grain structure with the geometry of the crank. This results in significantly improved strength, fatigue resistance, and toughness — all of which are critical for the high-load demands of automotive diesel engines. For this reason, Force Motors uses forging exclusively for its production crankshafts.

The process begins with induction-heating each billet to approximately 1,350°C, followed by precision forging using between 150-250 tons of pressure to generate the basic web and journal geometry—including built-in counterweight profiles that approximate the required internal balance. Immediately after forging, each crankshaft undergoes a controlled normalizing cycle to refine grain structure, then is cooled at a controlled rate to achieve a tensile strength above 850-1000 MPa and more importantly, maintain dimensions.

Next, the roughly forged crank has a buffer of 3 mm for machining. This part is also then shot blasted, and excess is trimmed. Before moving on to machining the part, it is crack tested and checked for defects. There are also other tests to check if the forging has left the material in a desirable condition, such as hardness testing.

The crankshaft is then machined on multi-axis CNC lathes and milling centres to remove excess material, establish journal diameters and oil-passage profiles. Any scales created during the machining process is removed by the means of sandblasting and pickling. Another specific requirement is polishing the oil holes for better, unrestricted fluid flow.

All crankshafts are finally dynamically balanced to cancel out any error in manufacturing, causing the part to deviate from its theoretical design. Crankshafts are balanced within an accuracy of 250 *gm · mm*. Finally, the crankpins and main journals, the parts that are going to be in constant contact with other metal parts, are fine lapped to create a precise and smooth surface finish.

### **Importance of precision in high-speed operation**

At high engine speeds, the crankshaft is subjected to rapidly fluctuating loads, significant inertial forces, and high-frequency torsional vibrations. Under such conditions, even minute deviations in geometry—such as journal ovality (run away), misalignment, or most significantly, unbalanced rotational mass—can lead to amplified dynamic stresses and premature failure.

Precision in crankshaft design, balancing and manufacturing ensures that critical parameters are within the required tolerances to function safely, and as intended. This report addresses all of these mechanical limitations and requirements of a crankshaft to ensure smooth and long-lasting crankshafts.

## Working Principle

From a kinematics perspective, the core of an internal combustion engine's power transmission is a classic slider-crank mechanism. This mechanism is the fundamental system responsible for the interconversion of linear and rotary motion, translating the immense force generated during combustion into the usable torque that power the vehicle.

The assembly consists of three primary bodies:

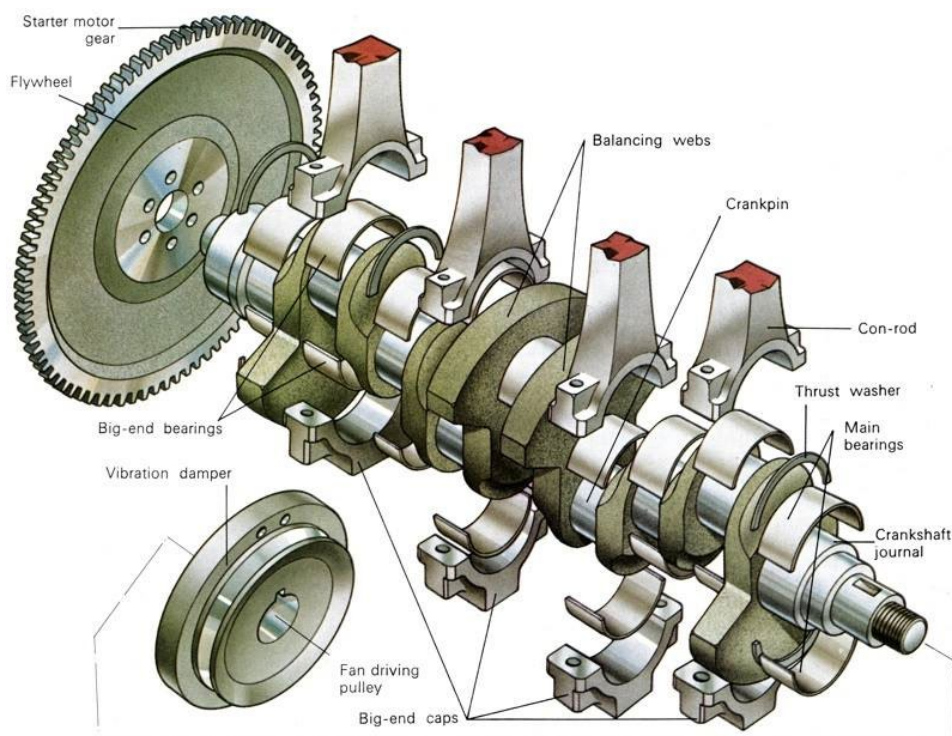


*Figure 7: Annotated drawing of the different components part of a crank assembly*

1. The crank: This is the rotating element of the mechanism. In this context, the “crank” is the specific section of the crankshaft assembly comprising the two crank webs and the offset crankpin. It rotates around a fixed axis defined by the main journals.
2. The coupler: This is the link that connects the crank to the slider. The connecting rod (conrod) serves as the coupler in this system. It has two pin joints, one at the crankpin (the “big end”) and one at the piston (the “small end”), allowing it to translate the motion between them
3. The slider: This is the component constrained to linear, reciprocating motion. The piston, moving within the fixed path of the cylinder, acts as a slider.

The conversion of motion is governed by the geometry of this linkage. As the piston is driven downwards by combustion pressure, the linear force is transmitted through the connecting rod

to the crankpin. Because the crankpin is offset from the crankshaft's main rotational axis by a distance  $r$  (the crank radius), this force creates a torque ( $T = F \times r \sin(\theta)$ ) that drives the rotation of the crankshaft. Conversely, on the non-power strokes (intake, compression, exhaust), the stored rotational inertia of the crankshaft moves the crank, which in turn drives the piston up and down, allowing it to complete its cycle while only having momentum being created in  $\frac{1}{4}$  of the duration of the cycle.

The dynamic forces acting on this mechanism are a combination of two primary sources that vary with the crank angle:

1. Gas Pressure Forces ( $F_g$ ): The high magnitude force generated by the combustion process within the cylinder, pushing down directly from the piston crown.
2. Inertia Forces ( $F_i$ ): The forces that arise from the constant acceleration and deceleration of the reciprocating masses. This occurs as the piston (and the parts connected to it), keep switching directions of motion, causing them to have an inertial force that cannot be overlooked.

The understanding of the cause of these forces, as well as the time of the cycle at which they act are paramount when trying to design and balance a well-functioning and long-lasting crankshaft. Depending on the loading situation and crank angle, the way these forces act on the crankshaft change in  $720^\circ$  cycle, creating complex loading scenarios that the crankshaft needs to be designed to withstand.

# **Crankshaft Design Guideline**

## **Loading Scenarios During Combustion**

A well-engineered crankshaft is designed while keeping in mind the various loading conditions it must withstand, repetitively. Due to the large amounts of forces exerted on the crankshaft and its components through the combustion process, ensuring its smooth function without breaking or cracking can be a challenge. To get an idea of the limiting variables in design, the various loading conditions acting on different parts of the crankshaft are determined:

### **1. Crankpin**

- a. **Bearing Pressure limitation:** The crankshaft experiences forces transmitted from the combustion chamber through the connecting rod, resulting in bearing pressure on the crankpin. The calculations for the dimensions of the crankpin are highly dependent on this pressure.
- b. **Shear Stress:** The crankpin experiences shear stress at the junction with the webs, where the combustion force attempts to shear off the pin. As it is connected on both ends, the surface area is taken accordingly.
- c. **Bending Stress:** Additionally, the crankpin experiences bending stress due to the combustion force acting at the midpoint, analogous to a simply supported beam scenario.

### **2. Crank web**

- a. **Compressive Force:** When the piston is at TDC, and there is ignition in the combustion chamber, a large force is pushing the crank web downwards. Again, as there are two crank webs for every crankpin (which translates this force), half the force acts on each web.
- b. **Twisting Force:** Once the Crank web is at an angle, the same force acts perpendicular to its length, causing it to bend and twist.

### **3. Crank Shaft**

- a. **Bending Stress:** There is pure bending when the piston is in TDC, where the force is acting directly above the crankshaft. Again, it mimics a simply supported beam.
- b. **Torsional Stress:** When the crankpin is at an angle to the shaft, it creates a torque that twists the shaft along its rotational axis.

## Crankshaft Dimensional Constraints Based on Mechanical Limits

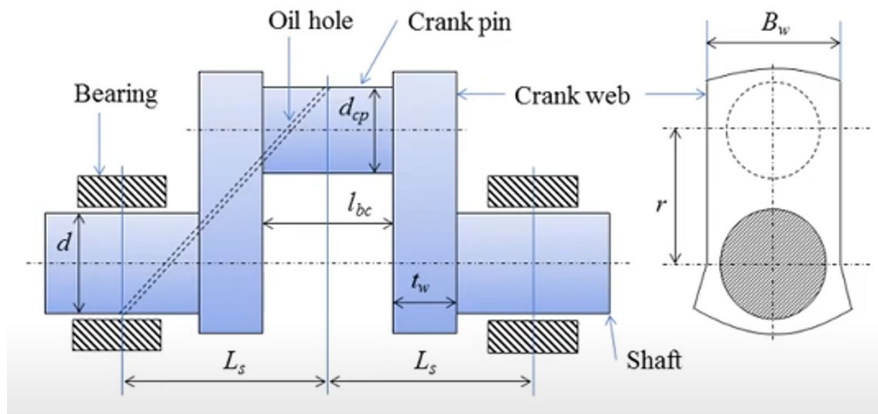


*Figure 8: Dimensioned Drawing of Crankshaft*

This section aims to translate the previously defined loading conditions into specific geometric design constraints for the crankshaft's primary components. By applying fundamental principles of solid mechanics and using the defined mechanical properties of 38MnVs6 steel, the following calculations determine the minimum permissible dimensions for the crankpin, crank webs, and main shaft. The goal is to ensure the component's structural integrity under the peaking bearing pressure, shear stresses and other loading conditions that were defined above. All the variables used in the upcoming calculations are listed in Table 1.

Table 1: Definitive list of all variables used in calculations (nomenclature)

Context	Variable	Description	Unit
Force Inputs	$F_{g,max}$	Peak Combustion Force	N
	$F_{g,avg}$	Average Combustion Force	N
	$F_i$	Inertial Force	N
	$F$	Force transmitted by Conrod	N
Derived Parameters and known Geometric Inputs	$L_{cp}$	Crankpin Axial Length	mm
	$d_{cp}$	Crankpin Diameter	mm
	$A_s$	Crankpin Cross-Sectional Area under Shear	Mm <sup>2</sup>
	$M_b$	Maximum Bending Moment	N·mm
	$I_{cp}$	Crankpin MOI	mm <sup>4</sup>
	$I_w$	Crank web MOI	mm <sup>4</sup>
	$y_{cp}$	Distance from Crankpin Neutral Axis	mm
	$y_w$	Distance from Crank Web Neutral Axis	mm
	$y_{mj}$	Distance from Main Shaft Neutral Axis	mm
	$t_w$	Crank web thickness	mm
	$d_{mj}$	Main Journal Diameter	mm
	$L_s$	Main Shaft Length	mm
	$B_w$	Crank web breadth	mm
	$\theta$	Crank Angle	° Degrees 

The value of  $F_{g,max}$  is derived from the peak firing pressure in the combustion chamber using the simple equation:

$$F = P \times A \quad (\text{Equation 1})$$

Where:

$$P = 150 \text{ bar} = 15 \text{ N/mm}^2$$

$$A = 4357.661 \text{ mm}^2 \text{ (piston crown area derived from CAD model)}$$

That gives a value of:

$$F_{g,max} = 65,394.92 \text{ N}$$

## 1. Crankpin

### a. Bearing Pressure:

The dimensions of the crankshaft are directly dependent on the maximum allowable combustion force  $F_{g,max}$ . However, when looking at the bearing pressure, it is a lot more feasible for manufacturing to look at the average gas force acting on the crankpin instead of the worst-case situation. For this reason, we use  $F_{g,avg}$  which is related to  $F_{g,max}$  as shown below:

$$F_{g,avg} = 0.4 \times F_{g,max}$$

$$F_{g,avg} = p_b \times L_{cp} \times d_{cp} \quad (\text{Equation 2})$$

The permissible bearing pressure varies with lubrication, but for the Pressure lubricated bearings used by Force Motors:

$$p_b = 10 - 12 \text{ N/mm}^2$$

(Equation 2) can be rearranged to identify permissible crankpin dimensions:

$$L_{cp} = \frac{F_{g,avg}}{p_b \times d_{cp}} \quad (\text{Equation 3})$$

### b. Shear Stress:

$$A_s = 2 \times \frac{\pi \times d_{cp}^2}{4} = \frac{\pi \times d_{cp}^2}{2}$$

Thus, the shear stress acting on the crankpin is:

$$\tau = \frac{F_{g,max}}{\pi \times d_{cp}^2}$$

To ensure structural integrity, this shear stress must remain below the allowable shear stress of the crankpin material (38MnVs6 high-strength steel):

$$\tau \leq \tau_{all}$$

Where:

$$\tau_{all} = 200 \text{ N/mm}^2$$

Rearranging to determine the minimum allowable crankpin diameter:

$$d_{cp} \geq \sqrt{\frac{2 \times F_{g,max}}{\pi \times \tau_{all}}} \quad (\text{Equation 4})$$

### c. Bending Stress

The maximum bending moment  $M_b$  for a point load:

$$M_b = \frac{F_{g,max} \times L_{cp}}{8}$$

The bending stress  $\sigma$  is calculated using the crankpin's cross-sectional geometry. The crankpin's section modulus is determined using the moment of inertia and the distance from the neutral axis  $y_{cp}$ :

$$I_{cp} = \frac{\pi \times d_{cp}^4}{64}, \quad y_{cp} = \frac{d_{cp}}{2}$$

And,

$$\sigma = \frac{4 \cdot F_{g,max} \cdot L_{cp}}{\pi \cdot d_{cp}^3}$$

Again, to ensure structural integrity, the tensile stress must be less than the allowable tensile stress of the steel:

$$\sigma \leq \sigma_{all}$$

Where:

$$\sigma_{all} = 350 \text{ N/mm}^2$$

Rearranging gives this:

$$L_{cp} \leq \frac{\pi \cdot \sigma_{all} \cdot d_{cp}^3}{4 \cdot F_{g,max}} \quad (\text{Equation 5})$$

To help visualize this and see the range of acceptable values, these three equations ((Equation 3), (Equation 4), &(Equation 5) are plotted on a coordinate system, with  $d_{cp}$  along the vertical and  $L_{cp}$  along the horizontal.

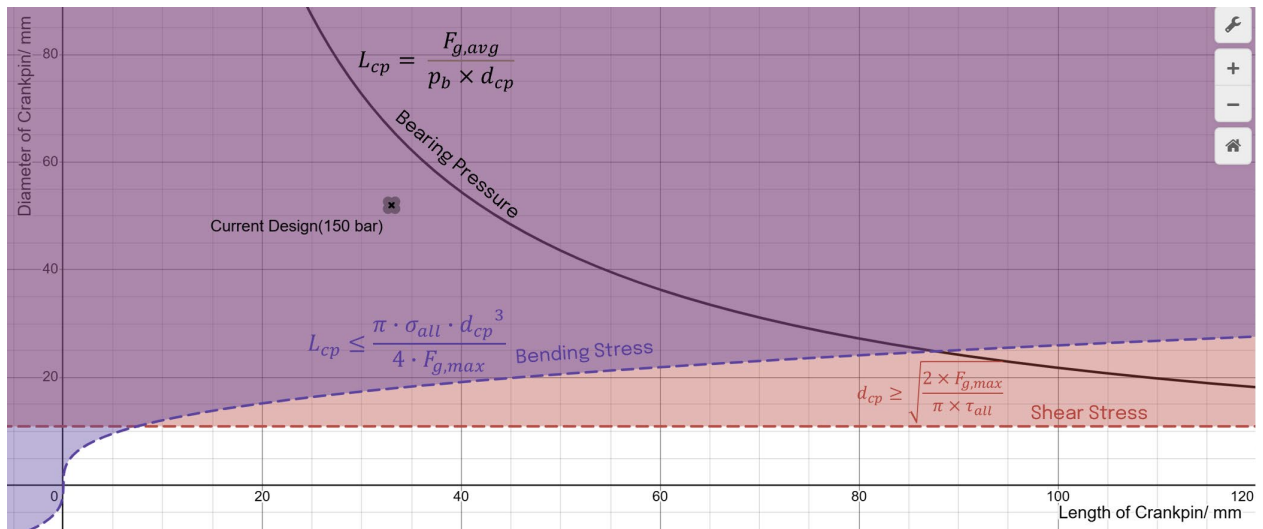


Figure 9: Graph Representing allowable diameter and length of crankpin

## 2. Crank Web

### a. Compressive Stress

The crank web is subjected to maximum compressive stress when the piston is at Top Dead Centre (TDC) and combustion pressure is at its peak. The axial gas force acts through the connecting rod and transfers to the crank web via the crankpin. As there are crank webs attached to each crankpin,  $F_{g,max}$  is evenly distributed between each. And the area resisting this compressive stress is:

$$Area = d_{cp} \cdot t_w$$

This makes the compressive stress:

$$\sigma = \frac{F_{g,max}}{2 \cdot d_{cp} \cdot t_w}$$

Now to rearrange for the dimension we need,  $t_w$ :

$$t_w \geq \frac{F_{g,max}}{2 \cdot d_{cp} \cdot \sigma_{all}} \quad (\text{Equation 6})$$

### b. Bending Stress

When the crank angle  $\theta$  and conrod make a right angle, such that all the force from the piston is perpendicular to the length of the crank web, the twisting force is maximum. A heavy bending stress is created due to the offset between the crankpin and the main journal. So, the bending moment on the web is found by:

$$M_b = F \cdot \left(r - \frac{d}{2}\right), \quad \sigma_{all} = \frac{M_b \cdot y_w}{I_w}$$

Where the inertia for two crank webs is:

$$I_w = 2 \cdot \frac{1}{12} \cdot t_w \cdot B_w^3, \quad y_w = \frac{B_w}{2}$$

The value of  $F$  is found by first computing the resultant force acting from the piston, which includes inertia, and then the component in the direction of the con rod is determined as follows:

$$F_r = F_{g,\theta} + F_i$$

Where  $F_i$  is the inertia of the total reciprocating mass. To avoid swaying from the focus of this project, the double derivation of the acceleration of the reciprocating mass is not added. Instead:

$$F_i = m_{res} \cdot (r\omega^2 \cdot \cos(\theta) + \frac{2r^2\omega^2}{l} \cdot \cos(2\theta))$$

And the value of the gas force is assumed to use a cosine curve for simplicity but before that, the value of  $\theta$  that is the point at which the right angle is created can be found using simple trigonometry:

$$\tan(\theta) = \frac{l}{r}$$

The two values are determined from the CAD:

$$l = 145.2 \text{ mm}$$

$r = 50 \text{ mm}$  (crank throw)

This gives a value of  $\theta$ :

$$\theta = 70.98^\circ$$

The equation for modelling a cosine curve of the power stroke of an engine is this, plugging the previously determined value of  $\theta$ :

$$F_{g,\theta} = F_{g,max} \cdot \cos(\theta)$$

$$F_{g,\theta} = 21,302.3 \text{ N}$$

Now to get  $F$  from the  $F_r$  just determined, the use of trigonometry is again applied:

$$F = \frac{F_r}{\sin(\theta)}$$

$$F = 22,532.5 \text{ N}$$

After substituting, simplifying and rearranging the equation:

$$B_w \geq \sqrt{\frac{3 \cdot F \cdot \left(r - \frac{d_{mj}}{2}\right)}{t_w \cdot \sigma_{all}}} \quad (\text{Equation 7})$$

As done previously for the crankpin design limitations, here is a graph representing an allowable range by plotting (Equation 6) and (Equation 7).

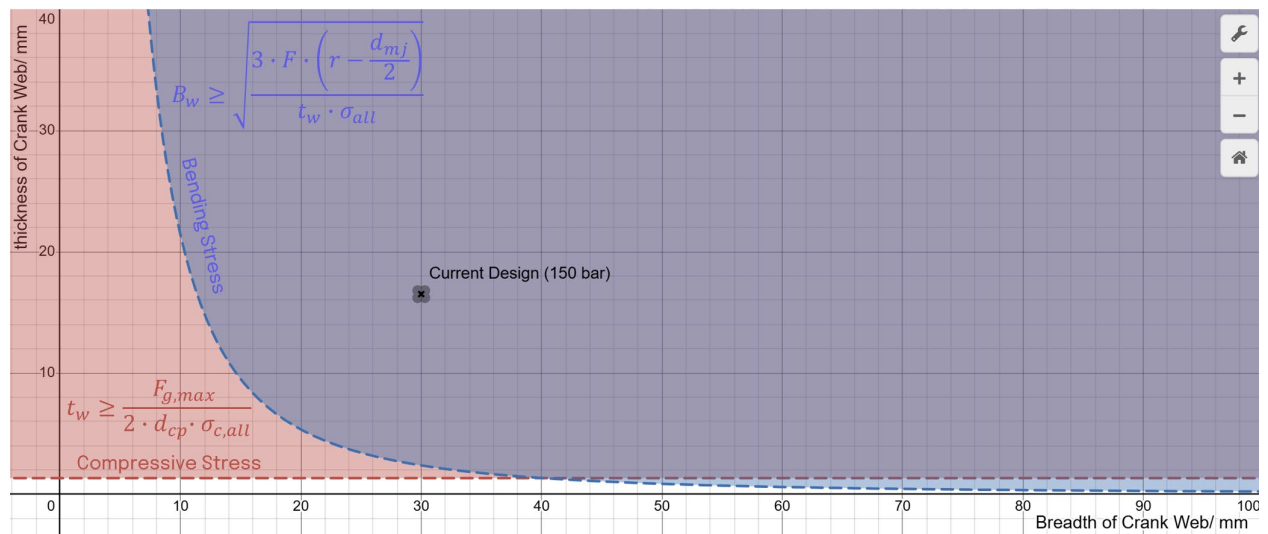


Figure 10: Graph Representing allowable thickness and breadth of Crank Web

### 3. Main Shaft

#### a. Bending Stress

When the crankpin and main journal are vertically aligned, at TDC,  $F_{g,max}$  acts directly on the main journal, creating a pure bending situation. So:

$$\sigma = \frac{M_b \cdot y_{mj}}{I_{mj}}$$

The bending moment, distance from centroid and MOI on the shaft are calculated as:

$$M_b = \frac{F_{g,max} \cdot 2L_s}{4}, \quad y_s = \frac{d_{mj}}{2}, \quad I_s = \frac{\pi}{64} \cdot d_{mj}^4$$

Substituting gives:

$$\sigma = \frac{16F_{g,max} \cdot L_s}{\pi \cdot d_{mj}^3}$$

This equation essentially defines the minimum journal diameter to withstand bending from peak cylinder pressure. However, all calculated values need to account for the allowable tensile stress:

$$\sigma \leq \sigma_{all}$$

Finally, after rearranging:

$$d_{mj} \geq \left( \frac{16F_{g,max} \cdot L_s}{\pi \cdot \sigma_{all}} \right)^{1/3} \quad (\text{Equation 8})$$

b. Torsional Stress:

When the crank web and connecting rod are at a right angle, the torsional force trying to twist the crankshaft along its length is maximum. The shaft, in this situation, experiences bending and torsion.

The torque and bending respectively experienced are:

$$T = \frac{F}{2} \cdot r, \quad M = \frac{F \cdot L_s}{2}$$

The equivalent torque is:

$$T_e = \sqrt{M^2 + T^2}$$

The shear stress due to this torque can be given as:

$$\tau = \frac{16 \cdot T_e}{\pi \cdot d_{mj}^3}$$

Including the allowable shear stress and rearranging:

$$d_{mj} \geq \left( \frac{8F_{g,90^\circ} \sqrt{L_s^2 + r^2}}{\pi \cdot \tau_{all}} \right)^{1/3} \quad (\text{Equation 9})$$

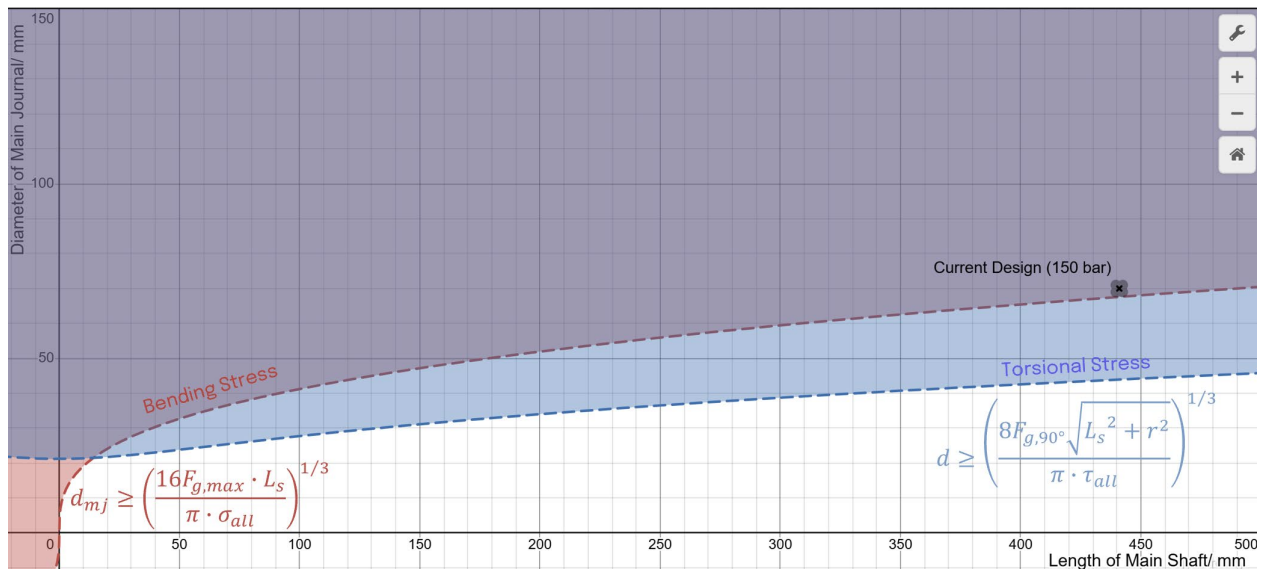


Figure 11: Graph Representing allowable diameter and length of Main Shaft

# Crankshaft Balancing

## Principles of Unbalance: Static and Dynamic Balancing

The unbalance within a rotating system like a crankshaft can be resolved into two fundamental forms: **static unbalance** and **couple unbalance**. The presence of either or both of these results in a state of **dynamic unbalance**, which generates undesirable vibrations and forces on the engine block.

### 1. Static Unbalance

Static unbalance occurs when the principal axis of inertia of the rotating body is displaced parallel to the axis of rotation. Simply put, the crankshaft's centre of mass is not located on its rotational centreline. This creates a net centrifugal force that attempts to move the axis of rotation away from its current axis, causing a vibration. When the crankshaft is at rest, this unbalance will cause it to rotate until the heavy spot is at the lowest point.

The magnitude of static unbalance is measured as the product of the unbalance mass and its radial distance from the axis of rotation ( $m \cdot r$ ). Correction is achieved by adding an equal counterweight directly opposite ( $180^\circ$ ) to the unbalance mass, which realigns the center of mass with the axis of rotation.

### 2. Couple Unbalance

Couple unbalance exists when there are two equal and opposing unbalance forces located at different points along the crankshaft's axis. Even if the crankshaft is statically balanced (meaning the combined centre of gravity is on the rotational axis), these two forces create a "couple" or a "rocking moment." This moment attempts to tilt the crankshaft, causing it to wobble end-to-end around its centre of mass.

This condition cannot be corrected by a single counterweight. It requires corrective masses to be placed in at least two separate planes along the crankshaft to create an opposing couple that cancels out the rocking moment. The magnitude of a couple unbalance is calculated as the product of the unbalance force and the axial distance separating the two forces ( $m \cdot r \cdot l$ ). From this, it is easy to understand why individually balanced crankshafts are preferred. There are more points (counterweights) within the length of the crankshaft itself to balance out these couples, whereas in an assembly balanced crankshaft, the middle is still trying to flex and wobble. In the process, a lot of internal stresses are applied on the main journal.

### 3. Dynamic Unbalance

Dynamic unbalance is the most general state and is a combination of both static and couple unbalance. In this condition, the principal axis of inertia is neither parallel to nor intersecting the axis of rotation. This is the state found in most real-world rotating systems before balancing. It results in both a net centrifugal force and a rocking moment, creating complex vibrations throughout the engine's operating range. To achieve a complete dynamic balance, both the net forces and the net couples must be eliminated, which requires making corrective adjustments in at least two separate planes along the crankshaft.

#### Assumptions & Notes

The following assumptions were made to establish the analytical framework for the crankshaft balancing calculations:

1. Rigid Body Assumption: All components are treated as perfectly rigid bodies.
2. Connecting Rod Mass Distribution: Mass is simplified into two discrete point masses...
3. Uniform Density & Geometry
4. Negligible Friction
5. Exclusion of External Components
6. Coordinate System Definition

#### Analytical Model for the balancing of Individually Balanced Crankshaft

The following analytical model was developed to calculate the inherent unbalance in the 4-cylinder crankshaft and to subsequently design the necessary counterweights for an individual balance. The process involves quantifying the existing unbalance, which is derived from the component's solid model, and then introducing an opposing counterbalance.

#### **Quantifying Inherent Unbalance**

First, the unbalance generated by each rotating component (crank webs, crankpins) and the simulated reciprocating masses (bob weights) are calculated. The **Mass and Centre of Gravity (CoG)** for each component were precisely determined from the 3D CAD model in CATIA. The model was digitally sectioned to isolate each part for individual measurement.

Based on each component's mass, CoG, and angular position, the static unbalance (force) and couple unbalance (moment) are resolved into their respective X and Y components. The total unbalance for the system is found by summing these individual vectors.

Table 2: Static Unbalance Contributions from Crankshaft Components

Part	Mass grams	CoG/ mm		Crank Angle / (Degrees °)	Static Unbalance		
		x	y		Resultant	x	y
web 1	789.00	0.040	30.458	0.08	24031.15	24031.13	31.56
crankpin 1	536.00	-0.125	49.954	359.86	26775.43	26775.34	-67.00
bob weight 1	1395.05	-0.125	49.954	359.86	69688.55	69688.33	-174.38
web 2	731.00	0.000	30.507	0.00	22300.62	22300.62	0.00
web 3	718.00	-0.080	-31.673	180.14	22741.29	-22741.21	-57.44
crankpin 2	536.00	0.125	-49.956	179.86	26776.50	-26776.42	67.00
bob weight 2	1395.05	0.125	-49.956	179.86	69691.34	-69691.12	174.38
web 4	765.00	0.000	-30.544	180.00	23366.16	-23366.16	0.00
web 5	768.00	-0.041	-31.102	180.08	23886.36	-23886.34	-31.49
crankpin 3	536.00	0.125	-49.954	179.86	26775.43	-26775.34	67.00
bob weight 3	1395.05	0.125	-49.954	179.86	69688.55	-69688.33	174.38
web 6	715.00	-0.038	-31.082	180.07	22223.65	-22223.63	-27.17
web 7	734.00	0.040	31.088	0.07	22818.61	22818.59	29.36
crankpin 4	536.00	-0.125	49.956	359.86	26776.50	26776.42	-67.00
bob weight 4	1395.05	-0.125	49.956	359.86	69691.34	69691.12	-174.38
web 8	788.00	0.000	30.047	0.00	23677.04	23677.04	0.00
<b>Total Unbalance</b>						<b>610.03</b>	<b>-55.18</b>

Table 3: Couple Unbalance Contributions from Crankshaft Components

Part	Distance from Central Journal	Couple Unbalance	
		x	y
web 1	-177.58	-5604.55	-4267543.36
crankpin 1	-152.88	10243.09	-4093468.14
bob weight 1	-152.88	26659.75	-10654090.92
web 2	-128.86	0	-2873635.21
web 3	-75.98	4364.35	1727900.18
crankpin 2	-51.88	-3475.96	1389160.46
bob weight 2	-51.88	-9046.9	3615575.19
web 4	-27.85	0	650747.56
web 5	27.41	-862.99	-654652.81
crankpin 3	52.12	3491.91	-1395477.38
bob weight 3	52.12	9088.40	-3632016.26
web 6	76.13	-2068.56	-1691973.85
web 7	129.01	3787.73	2943826.55
crankpin 4	153.12	-10259.04	4100004.82
bob weight 4	153.12	-26701.26	10671103.96
web 8	177.73	0	4208001.22
<b>Total Unbalance</b>		<b>-384.02</b>	<b>43462.03</b>

### Designing the Counterbalance

Next, counterweights are designed to generate an opposing static and couple balance. The mass and CoG of each counter web are determined from their CATIA models to create forces and moments that directly counteract the unbalance calculated in the previous step.

Table 4: Static balancing from Crankshaft Counter webs

Part	Mass /g	CoG/ mm		Crank Angle / (Degrees °)	Static Unbalance/ g · mm		
		x	y		Resultant	x	y
Counterweb 1	1019.0	-0.002	-30.933	180.00	31520.7	-31520.73	-2.04
Counterweb 2	992.0	0.000	-30.950	180.00	30702.4	-30702.40	0.00
Counterweb 3	920.0	0.000	32.600	0.00	29992.0	29992.00	0.00
Counterweb 4	1004.0	0.000	32.600	0.00	32730.4	32730.40	0.00
Counterweb 5	1004.0	0.000	32.600	0.00	32730.4	32730.40	0.00
Counterweb 6	920.0	0.000	32.600	0.00	29992.0	29992.00	0.00
Counterweb 7	992.0	0.000	-30.950	180.00	30702.4	-30702.40	0.00
Counterweb 8	1070.0	0.000	-30.950	180.00	33116.5	-33116.50	0.00
<b>Total Unbalance</b>						<b>-597.23</b>	<b>-2.04</b>

Table 5: Couple Unbalance from Crankshaft Counter webs

Part	Distance from Central Journal	Couple Unbalance	
		x	y
Counterweb 1	-178.44	363.66	5624495.48
Counterweb 2	-128.22	0.00	3936723.13
Counterweb 3	-76.69	0.00	-2300026.50
Counterweb 4	-26.47	0.00	-866471.88
Counterweb 5	26.56	0.00	869384.88
Counterweb 6	76.78	0.00	2302695.78
Counterweb 7	128.31	0.00	-3939455.65
Counterweb 8	178.53	0.00	-5912222.51
<b>Total Unbalance</b>		<b>363.66</b>	<b>-284877.25</b>

### Final Balancing

Looking at the resultant unbalance after the shaft is internally balanced using counter webs. The table below represents the remaining unbalance

Table 6: Total Remaining Unbalance

	Static Unbalance			Couple Unbalance		
	x	y	Resultant	x	y	Resultant
Resultant	12.80	-57.22	<b>58.63</b>	-20.36	153.42	<b>154.77</b>

**Balancing Rate:** The final Balancing Rate is calculated to be **49.6%**. This indicates a highly effective counterbalance design that neutralizes most of the inherent static unbalance. The value of  $58.63 \text{ g} \cdot \text{mm}$  is significantly lower than the accepted value of  $250 \text{ g} \cdot \text{mm}$ .

## Crankshaft Fatigue Testing for Validation

Prior to full scale production, prototype crankshafts undergo rigorous fatigue testing to validate the design's durability under simulated, accelerated operating loads. This testing is carried at the Automotive Research Association of India (ARAI) Chakan, for Force Motors.

Test specimens are prepared from a 4-cylinder prototype crankshaft. The crankshaft is sectioned to isolate a single crankpin situated between two main journals, which is then mounted in a test fixture. To evaluate the entire crankshaft, two prototypes are typically supplied; specimens from the 1<sup>st</sup> and 3<sup>rd</sup> crankpins are taken from the first crankshaft, while the 2<sup>nd</sup> and 4<sup>th</sup> crankpins are taken from the second. A load is exerted on the journal using a mechanically actuated pulsator, which is powered by springs. An image of the setup jig ( Figure 12) and an image of the pulsator are attached below (Figure 13).



*Figure 12: Image of the pulsator setup*      *Figure 13: Image of a High Frequency Pulsator*

The standard test protocol simulates loads experienced during engine operation. Loads are exerted in a cyclic manner, alternating between tensile (18 kN) and compressive (55 kN). A frequency of 52 Hz is used and its run for a target of 5 million cycles or until component failure, whichever occurs first.

Following the test cycle, the specimen is examined for fatigue cracks. These are most likely to form at areas of high stress concentration, such as filleted edges connecting the crankpin to the crank web and the crank web to the main journal. Crack detection is performed using standard

Non-Destructive Testing (NDT) methods, like Dye Penetrant Inspection, which highlight any surface-level discontinuities. During the test, an abrupt drop in the pulsator's operating frequency is a key indicator of a component fracture, and the number of cycles at the point of failure recorded.

However, if there aren't any cracks or abnormalities observed, the part is considered to have passed and is moved on to being tested at a Factor of Safety that 0.5 higher than previous. This process is repeated until failure occurs.

The results of this test determine the next steps in the design process:

1. If the specimen survives a FS above 1.5 and below 2.5, the design is considered sufficient and safe for operation in high-load environments. This a green light to commence manufacturing.
2. If the specimen fails below a minimum threshold (e.g.,  $FS < 1.5$ ), the design is deemed insufficient. The physical failure location is then compared against FEA simulation results to identify and reinforce high stress areas.
3. If the specimen fails at a significantly high FS ( $> 3.0$ ), it indicates the component is over-engineered. This presents the opportunity for optimization to reduce component weight, which can lower production costs and improve vehicle efficiency.

As ARAI runs these tests, the preliminary input values of the tensile and compressive loads are generated via simulations. Here are the input parameters that are determined, and then passed on to ARAI to base the fatigue tests on:

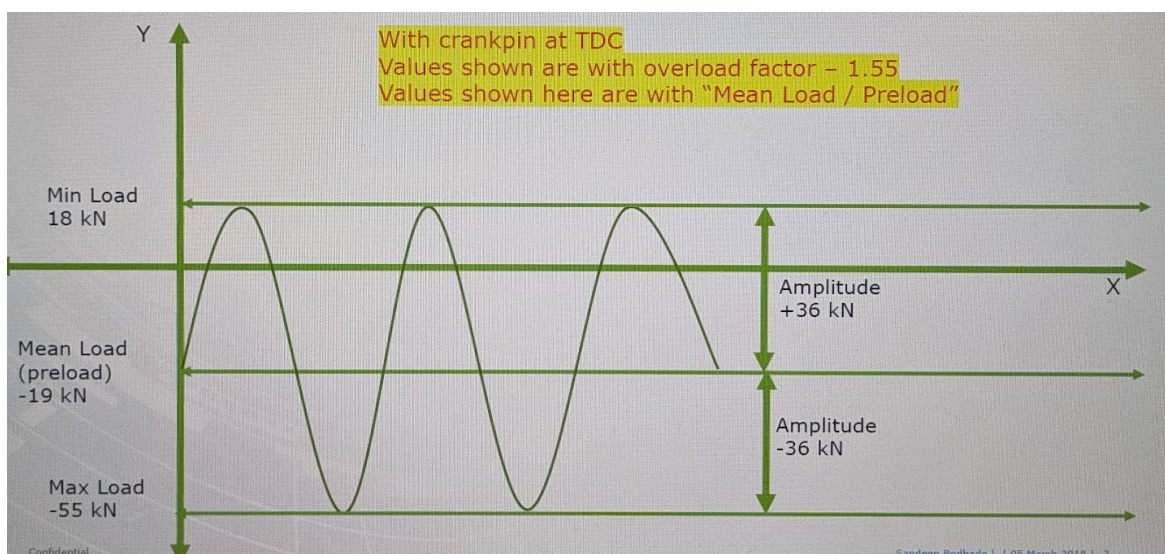


Figure 14: Fatigue Testing Input Data expressed as a function

Table 7: Input Data for ARAI Fatigue Testing

<b>Test Load – Con Rod (Big End)</b>		
Parameter	Value	Unit
Load Amplitude	75.44	kN
Mean Load	-50.73	kN
Load ratio	-5.10	[-]
Tensile Force (Pulse Test)	24.72	kN
Compressive Force (Pulse Test)	-126.17	kN
<b>Test Load – Con Rod (Small End)</b>		
Parameter	Value	Unit
Load Amplitude	75.44	kN
Mean Load	-58.89	kN
Load Ratio	-8.12	[-]
Tensile Force (Pulse Test)	16.55	kN
Compressive Force (Pulse Test)	-134.34	kN

Following this, a conclusive report is obtained from ARAI after the successful completion of the testing. As the fatigue test for the current 8 web crankshaft design is not completed, a conclusive report hasn't been generated and FML has only received the following report:

Table 8: Interim report on the Fatigue testing of 8-web Crankshaft

Sr. No.	Pin No.	FOS	Tensile Load (kN)	Compressive Load (kN)	Target Cycles	Test Status
1	3	1	18	-55	5 Million	Test completed
2	1	1	18	-55	5 Million	Test completed
3	2	1.5	27	-82.5	5 Million	Test completed
4	4	1.5	27	-82.5	5 Million	Test completed
5	3	2	36	-110	5 Million	Test completed
6	4	2	36	-110	5 Million	Test completed
7	2	2.5	45	-137	5 Million	Test completed
8	2	2.5	45	-137	5 Million	Test completed
9	2	3	54	-165	5 Million	Test completed
10	3	3	54	-165	5 Million	Sample failed at 175,284 cycles
11	3	3	54	-165	5 Million	Sample failed at 514,096 cycles
12	3	2.75	49.5	-151.25	5 Million	Test running

Below is a sample excerpt from a completed test report. However, it is for the 4 web crankshaft and is present just to provide an example for this paper: 

*Table 9: Test Results of Fatigue Testing Crankpins at different FS until failure*

Sr. No	Sample No	Pin ID	FOS	Tensile Load (kN)	Compressive Load (kN)	Target Million cycles	Remarks
1	SDL/12/2017/8505/1	Pin 1	1	18	-55	5	Passed. No visual failure observed. Refer Figure 15 for photograph after testing.
2	SDL/12/2017/8505/2	Pin 4	1	18	-55	5	Passed. No visual failure observed. Refer Figure 16 for photograph after testing.
3	SDL/12/2017/8505/3	Pin 1	1.5	27	-82.5	5	Passed. No visual failure observed. Refer Figure 17 for photograph after testing.
4	SDL/12/2017/8505/4	Pin 4	1.5	27	-82.5	5	Passed. No visual failure observed. Refer Figure 18 for photograph after testing.
5	SDL/12/2017/8505/5	Pin 1	2.0	36	-110	5	Passed. No visual failure observed. Refer Figure 18 for photograph after testing.
6	SDL/12/2017/8505/6	Pin 4	2.0	36	-110	5	Passed. No visual failure observed. Refer Figure 19 for photograph after testing.
7	SDL/12/2017/8505/7	Pin 1	2.5	45	-137.5	5	Failure observed at 1026788 cycles. Refer Figure 20 for failure photograph.
8	SDL/12/2017/8505/8	Pin 4	2.5	45	-137.5	5	Failure observed at 2524138 cycles. Refer Figure 21 for failure photograph.
9	SDL/12/2017/8505/9	Pin 1	2.25	40.5	-123.75	5	Failure observed at 1548806 cycles. Refer Figure 22 for failure photograph.
10	SDL/12/2017/8505/10	Pin 1	2	36	-110	5	Passed. No visual failure observed. Refer Figure 23 for photograph after testing.
11	SDL/12/2017/8505/11	Pin 4	2	36	-110	5	Failure observed at 2635961 cycles. Refer Figure 24 for failure photograph.
12	SDL/12/2017/8505/12	Pin 4	1.75	31.5	-96.25	5	Passed. No visual failure observed. Refer Figure 25 for photograph after testing.
13	SDL/12/2017/8505/13	Pin 3	1.75	31.5	-96.25	5	Failure observed at 4.52 million cycles. Refer Figure 26 for failure photograph.
14	SDL/12/2017/8505/14	Pin 2	1.75	31.5	-96.25	5	Passed. No visual failure observed. Refer Figure 27 for photograph after testing.
15	SDL/12/2017/8505/15	Pin 3	1.5	27	-82.5	5	Passed. No visual failure observed. Refer Figure 28 for photograph after testing.

16	SDL/12/2017/8505/16	Pin 2	1.5	27	-82.5	5	Passed. No visual failure observed. Refer Figure 29 for photograph after testing.
----	---------------------	-------	-----	----	-------	---	-----------------------------------------------------------------------------------

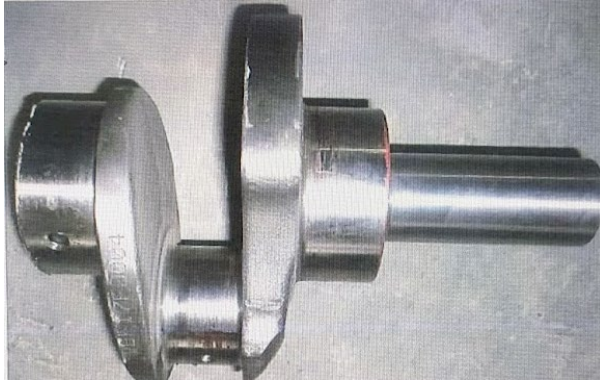


Figure 15: Image 1 from ARAI report

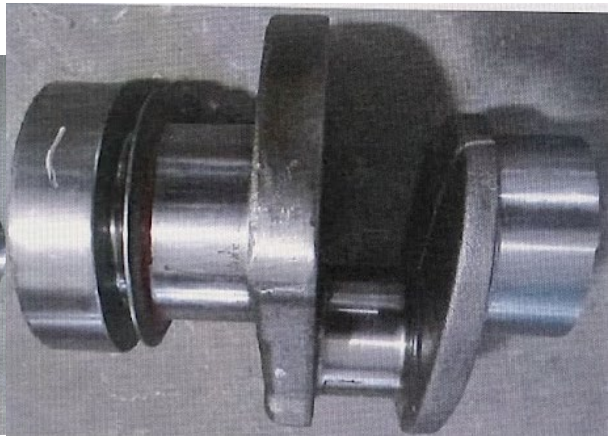


Figure 16: Image 2 from ARAI report



Figure 17: Image 3 from ARAI report



Figure 18: Image 4 from ARAI report

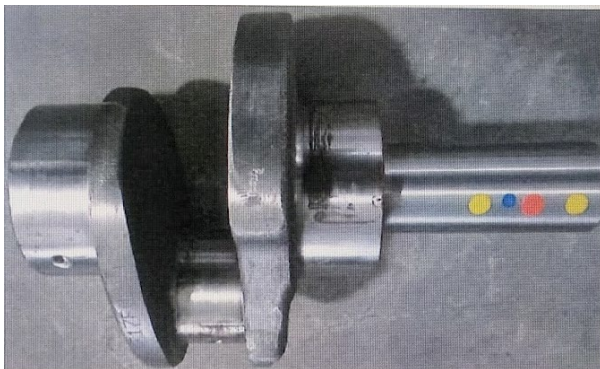


Figure 19: Image 5 from ARAI report

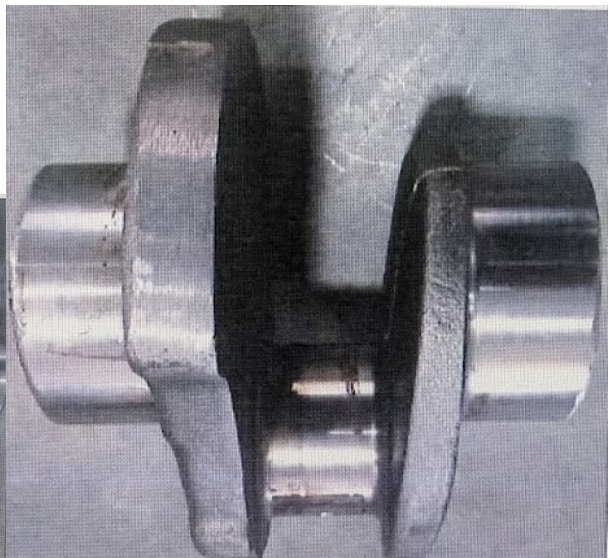


Figure 20: Image 6 from ARAI report



Figure 21: Image 7 from ARAI report



Figure 22: Image 8 from ARAI report



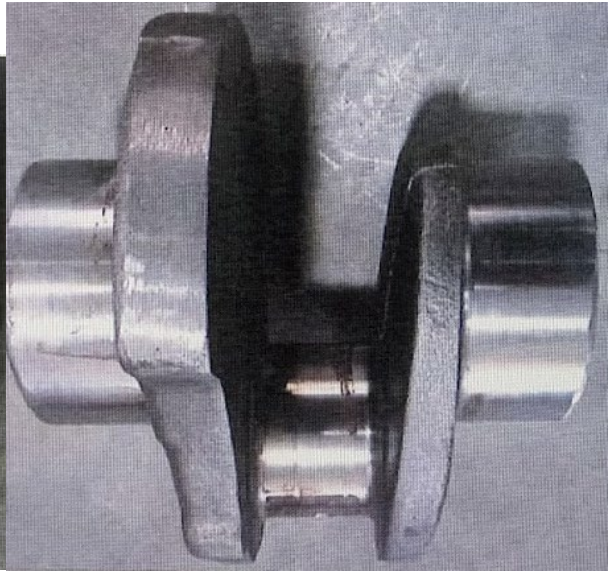
Figure 23: Image 9 from ARAI report



Figure 24: Image 10 from ARAI report



*Figure 25: Image 11 from ARAI report*



*Figure 26: Image 12 from ARAI report*



*Figure 27: Image 13 from ARAI report*

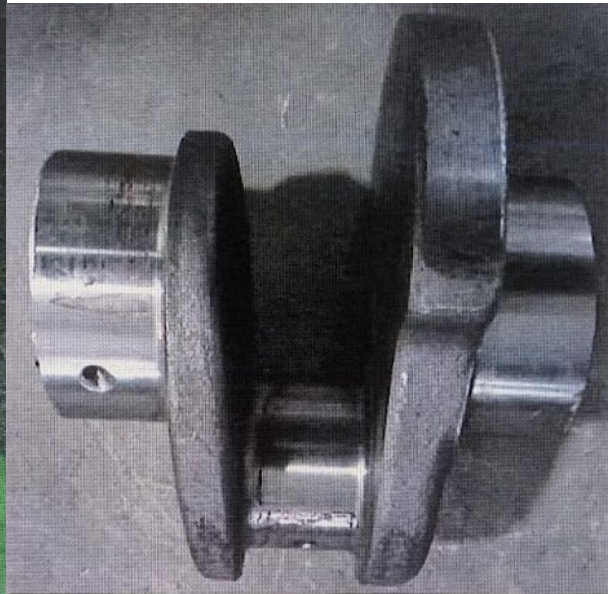


*Figure 28: Image 14 from ARAI report*

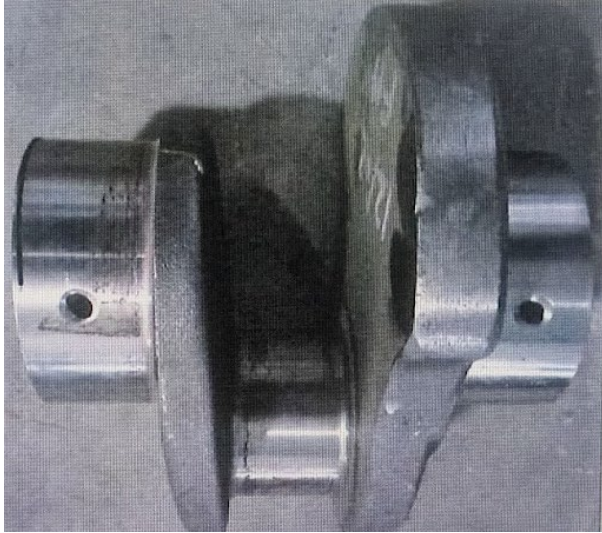


*Figure 29: Image 15 from ARAI report*

## Conclusion

The design and validation of the 4-cylinder, 150-bar individually balanced crankshaft presented in this report represents a comprehensive approach to solving dynamic balance and fatigue challenges in modern engine design. Through the application of analytical modeling, geometric constraint analysis, and real-world fatigue testing, this project has demonstrated that internally balanced crankshafts offer superior performance characteristics compared to traditional assembly-balanced systems.

Individually balancing the crankshaft through integrated counterweights not only reduced internal torsional stresses and vibration but also enabled modular assembly by eliminating the reliance on external balancing components. This design shift enhances interchangeability, simplifies manufacturing workflows, and contributes to long-term durability across a wider range of operating conditions.

The analytical model developed for calculating unbalance and counterweight design proved effective, achieving a final balancing rate of 49.6% — a result well within industry standards for dynamic balancing. Validation through fatigue testing at ARAI confirmed the design's robustness, with crankpins sustaining high cyclic loads across varying safety factors. Failures, when they did occur, aligned closely with simulation predictions, reinforcing the model's reliability.

Ultimately, this project highlights how precision engineering, when grounded in solid mechanical fundamentals and validated through empirical testing, can drive innovation in automotive powertrain systems. The individually balanced crankshaft design developed here offers Force Motors a scalable, high-performance solution suitable for next-generation diesel engines and sets a foundation for continued refinement in engine dynamics and manufacturing integration.